Stainless steel weld metal designed to mitigate residual stresses

Journal Item

Stainless steel weld metal designed to mitigate residual stresses

A. A. Shirzadi[1], H. K. D. H. Bhadeshia*[1], L. Karlsson[2] and P. J. Withers[3]

There have been considerable efforts to create welding consumables which on solid state phase transformation partly compensate for the stresses which develop when a constrained weld cools to ambient temperatures. All of these efforts have focused on structural steels which are ferritic. In the present work, alloy design methods have been used to create a stainless steel welding consumable which solidifies as δ ferrite, transforms almost entirely into austenite which then undergoes martensitic transformation at a low temperature of about 220°C. At the same time, the carbon concentration has been kept to a minimum to avoid phenomena such as sensitisation. The measured mechanical properties, especially toughness, seem to be significantly better than commercially available martensitic stainless steel welding consumables, and it has been demonstrated that the use of the new alloy reduces distortion in the final joint.

Keywords: Phase transformation, Residual stress, Stainless steel, Martensitic, Transformation plasticity

Introduction

Residual stresses are an anathema in welds because they are associated with distortion,[1–6] they limit the magnitudes of the external stress that a weld can support and influence the life of the joint in a variety of scenarios.[7–9]

There are a number of groups developing welding consumables capable of mitigating the residual stresses that develop when the liquid metal filling a joint solidifies and contracts.[10–24] The mechanism of stress cancellation relies on the solid state transformation of the weld metal into bainite or martensite at a sufficiently low temperature, such that the transformation plasticity cancels any strain due to thermal contraction. It is believed that the extent of this relief is dependent on the selection of crystallographic variants of the transformation product which are thermodynamically favoured in the particular environment of the accumulating residual stress.[25]

All previous work has focused on welding materials for ferritic steels containing relatively low concentrations of solutes. In contrast, the purpose of the present work was to develop a corresponding alloy for welding austenitic stainless steels. The weld metal must therefore contain a critical concentration of chromium in order to ensure a 'stainless' character through the spontaneous formation of a protective chromia film provided a trace of oxygen or oxidising agent is present. It must at the same time be able to transform into martensite at a relatively low temperature, so that the resulting plasticity can be exploited to compensate for any accumulated stress.

Design criteria

A suitable weld metal could be based on a martensitic stainless steel. Although such alloys are available commercially, it will be demonstrated later that they do not meet the set of requirements specified here:

(i) the chromium concentration must be maintained in excess of 12 wt-% to ensure the stainless character of the weld metal

(ii) the carbon concentration must be minimal to ensure toughness and to reduce the risk of precipitating chromium carbides[26–29]

(iii) from past experience, the martensite start temperature M_S must be kept low, in the range 150–250°C in order to ensure that the transformation is not exhausted before ambient temperature is reached. Otherwise thermal contraction leads to the accumulation of tensile stress as the weld continues to cool after transformation is exhausted.[10]

(iv) Since the carbon concentration must be minimised, other solutes have to be exploited to suppress M_S

(v) to fully exploit transformation plasticity, the alloy must be capable of becoming completely austenitic at high temperatures

(vi) the solidification of stainless steels is classified as austenitic or ferritic when the liquid completely freezes into one of these phases; two additional modes, austenitic–ferritic and ferritic–austenitic refer to the leading phase during solidification, with the trailing phase growing behind the main solidification front.[30–32] The hot cracking susceptibility of welds is greatly

[1]University of Cambridge, Materials Science and Metallurgy, Cambridge CB2 3QZ, UK
[2]ESAB AB, Central Research Laboratories, SE 40277 Göteborg, Sweden
[3]University of Manchester, School of Materials, Grosvenor St., Manchester M1 7HS, UK

*Corresponding author, email hkdb@cam.ac.uk

Published by Maney on behalf of the Institute
Received 27 February 2009; accepted 19 March 2009
DOI 10.1179/136217109X437178

affected by the solidification mode and the often unavoidable impurity content (S, P), with the greatest tendency to cracking occurring when austenite is the leading phase.[30–32] An important criterion is therefore to ensure that the designed alloy solidifies to δ ferrite. This condition limits the amount of austenite stabilising elements such as nickel that can be added to the weld metal.

Alloy design

Martensitic transformation begins when the free energy change $\Delta G^{\gamma\alpha}$ for austenite to change into ferrite of the same composition, equals a critical value $\Delta G_C^{\gamma\alpha}$.[33–37] The former value can be calculated using MTDATA[38] and the SGTE database; the critical free energy change, which depends on solute content, can be estimated from Ref 36. The method therefore allows the M_S temperature to be estimated as a function of chemical composition.

There is a difficulty in including silicon in the calculations since for stainless steels, the thermodynamic databases have been shown to lead to a gross overestimation of the δ ferrite content.[39,40] The silicon (<1 wt-%) was therefore neglected in the calculations. Indeed, a substantial improvement in the results was obtained when silicon was excluded from the list of accounted elements (Fe, C, Mn, Cr, Ni, Mo, P, S). The phases allowed are austenite, ferrite, cementite $M_{23}C_6$, M_7C_3, M_3C_2, and M_6C, where the 'M' stands for metal atoms. M_3C and M_2C are omitted because they are not, according to the calculations, stable phases at equilibrium.

In conducting the calculations the composition of a commercially available martensitic stainless coated electrode designated OK84·52, was used as a base and the compositions of candidate alloys were varied over the ranges listed in Table 1, bearing in mind the design criteria listed above. Figure 1 illustrates the influence of varying composition on the martensite start temperature. The required reduction in carbon concentration to less than 0·03 wt-% has the consequence of raising M_S to an unacceptably high value, so it has to be balanced using substitutional solutes. Although increasing the chromium concentration does reduce the M_S temperature, Fig. 2 shows that it then becomes impossible to get the fully austenitic state necessary to subsequently obtain a fully martensitic microstructure. The chromium content cannot of course be reduced to less than that in OK84·52 if the stainless character is to be maintained, so its concentration was maintained at 12·9 wt-% in all subsequent designs. Manganese and nickel are austenite stabilisers and after numerous calculations alloy 1 (1·5Mn–4Ni…) and alloy 2a (1·23Mn–6·12Ni…) were designed to be fully ferritic following solidification, and fully austenitic over a large temperature range above 1050 K, as illustrated in Fig. 3. The calculated equilibrium liquidus–solidus temperatures of alloys 1 and 2a are 1770–1750 K and 1760–1730 K respectively.

The sequence of alloy development and comparative studies is illustrated in Fig. 4 with details discussed later in the text.

Experimental alloys

Alloys were made as 800 g melts using a vaccum arc furnace having the chemical compositions listed in Table 1. Cylindrical samples of 8 mm diameter and 12 mm length were prepared for dilatometry using a Thermecmastor thermomechanical simulator. Each sample was austenitised at 1100°C for 10 min and then was cooled at a rate of 10 K s^{-1} to obtain a fully martensitic microstructure. The optical microstructures observed were martensitic and comparisons made against samples quenched in water or in liquid nitrogen from the austenitisation temperature confirmed this interpretation (Fig. 5).

An offset method[41,42] is used to ensure that M_S is determined objectively, i.e. independent investigators should reach the same conclusions given identical data. This is because the initiation of transformation is identified by a fixed strain of 1 vol.-% of martensite forming at room temperature.[41] The uncertainty of measurement is determined by the standard error in fitting a straight line to the dilatometric strain versus temperature curve before the onset of transformation.[41] Figure 6 shows typical results with the M_S temperatures determined to be 327 ± 13°C and 216 ± 2°C for alloys 1 and 2a respectively. The corresponding calculated values

Table 1 Chemical compositions (wt-%) of alloys studied*

	C	Cr	Ni	Mn	Mo	P	S	Si
Range studied theoretically	0·16–0·03	12·9–20·0	0·05–6·00	0·37–3·00	0·06–1·00	0·009	0·009	0·73
Alloy 1 (800 g melt)	0·01	12·9	4·00	1·50	0·06	0·009	0·009	0·73
Alloy 2a (800 g melt)	…	13·6	5·9	1·7	0·01	…	…	0·7
Alloy 2a single pass weld using 800 g melt	…	14·0	7·3	1·6	0·5	…	…	0·7
Austenitic stainless steel base plate	…	17·0	9·7	1·6	2·0	…	…	0·5
	C	Cr	Ni	Mn	Mo	P	S	Si
Metal cored alloy 2b multipass weld	0·014	12·66	5·24	1·36	0·10	0·002	0·006	0·76
Commercial martensitic multipass weld	0·013	11·99	6·20	1·06	1·39	0·002	0·006	0·71
	W	Nb	Cu	Al	Ti	B	O	N
Metal cored alloy 2b multipass weld	0·024	<0·001	0·01	0·027	0·053	0·0004	0·037	0·026
Commercial martensitic multipass weld	0·016	0·003	0·43	0·021	0·047	0·0006	0·034	0·026
	C	Cr	Ni	Mn	Mo	Cu	Si	
Austenitic solid wire OK Autrod 308LSi	0·03	19·5	10·0	1·8	…		0·8	…

*The first row shows the range of concentrations studied to calculate the M_S temperatures; the first number in each column of this row corresponds to a commercially available martensitic stainless steel welding alloy with the commercial designation OK84·52. Silicon was neglected as an input in the M_S calculations. The chemical compositions were determined using combustion analysis for all cases where the minor element (C,S,N,O) are reported, whereas the others were measured using energy dispersive X-ray analysis on a scanning electron microscope. The commercial metal cored martensitic alloy is a laboratory grade similar to OK Tubrod 15·53.

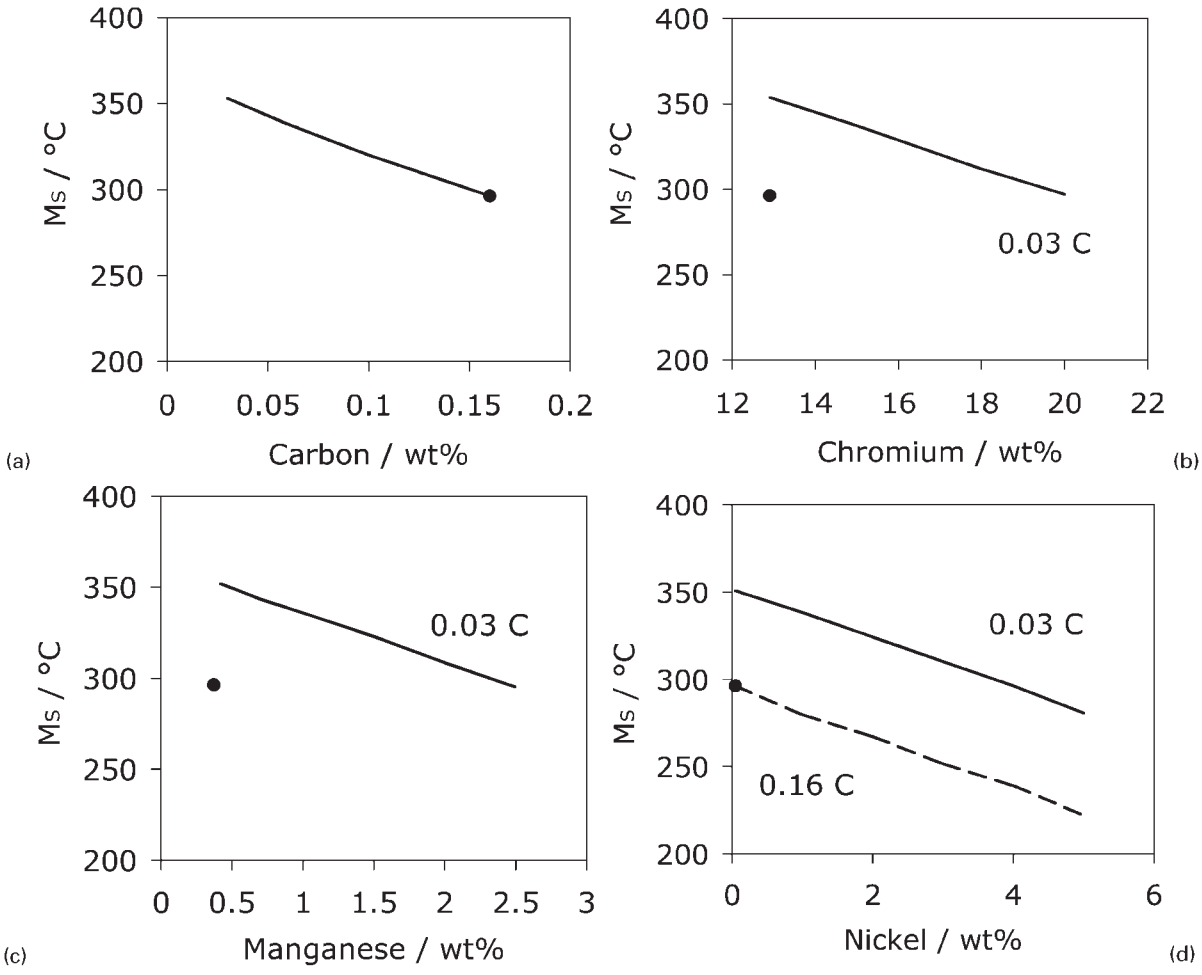

a effect of carbon; *b* effect of chromium; *c* effect of manganese; *d* effect of nickel at two levels of carbon

1 Calculated martensite start temperatures: single point in each figure represents commercial welding consumable OK84·52 (Table 1); where appropriate, carbon concentration used in calculations is indicated in wt-%

are somewhat different, with an underestimation in the case of alloy 1 (261°C) and overestimation in the case of alloy 2a (232°C). Further experiments were focused on alloy 2a with the lower measured transformation temperature.

Satoh test

This is a test designed to show the evolution of stress as a constrained sample cools from an elevated temperature.[43] A thermomechanical fatigue (TMF) testing machine was used for the Satoh test. Special adapters were designed to hold the rod shaped samples of alloy 2a with 3 mm diameter and 8 cm length in order to assess the capability of the alloy in mitigating the residual stresses. The samples were heated by induction up to 1100°C and kept at that temperature for about 2 min. The TMF machine was programmed to keep the

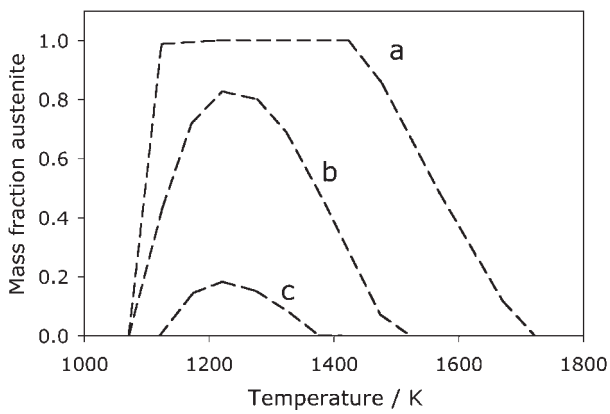

a OK84·52, 0·16C–12·9Cr–0·05Ni–0·37Mn–0·06Mo (wt-%); *b* OK84·52, 0·03C–12·9Cr–0·05Ni–0·37Mn–0·06Mo (wt-%); *c* OK84·52, 0·03C–16Cr–0·05Ni–0·37Mn–0·06Mo (wt-%)

2 Calculated austenite fraction as function of temperature: presence of silicon is neglected in these estimates

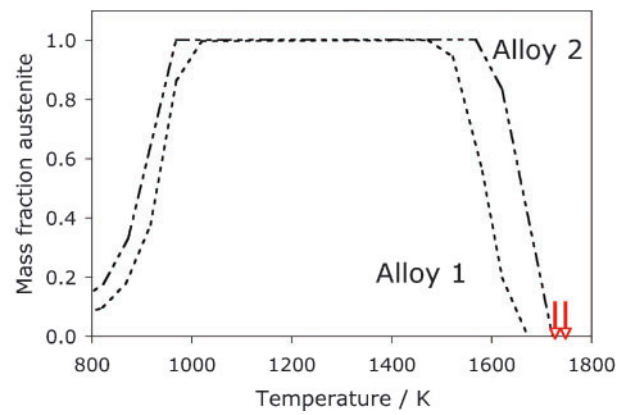

3 Calculated austenite content of alloy 1 (0·01C–12·9Cr–4Ni–1·5Mn, wt-%) and alloy 2a (0·01C–13Cr–6·12Ni–1·2Mn, wt-%): full compositions are listed in Table 1; two arrows on right are solidus temperatures, 1750 and 1730 for alloys 1 and 2a respectively

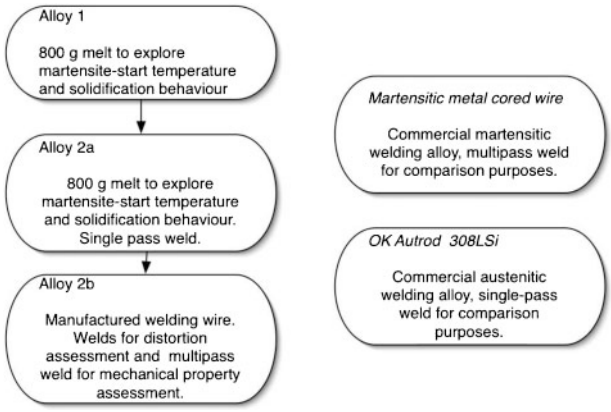

4 Sequence of alloy development and comparative studies (see also Table 1)

load at a zero level by compensating for the thermal expansion of the rods during heating. The grips of the machine were locked just before switching off the induction heating system. In order to maintain a fast cooling rate, compressed air was blown onto the sample until it reached room temperature.

It is important to note that there is a temperature gradient along the sample with the hottest part in the centre and coldest at the grips. The temperatures reported here are from a thermocouple attached to the centre of the sample, i.e. the hottest part. During cooling, phase transformation begins first in the part of the specimen which is away from the centre and hence the drop in stress due to transformation plasticity is recorded before the whole of the sample reaches the M_S temperature.

As can be seen from Fig. 7, tensile stress accumulates as the constrained sample cools from 1100°C. Martensitic transformation is stimulated on reaching about 280°C and the resulting transformation plasticity compensates for the accumulated stress, until the transformation is essentially exhausted. After that a small amount of stress accumulates due to the thermal contraction as the sample cools towards ambient temperature. This experiment shows the capability of the martensite in this stainless steel to act in the intended manner.

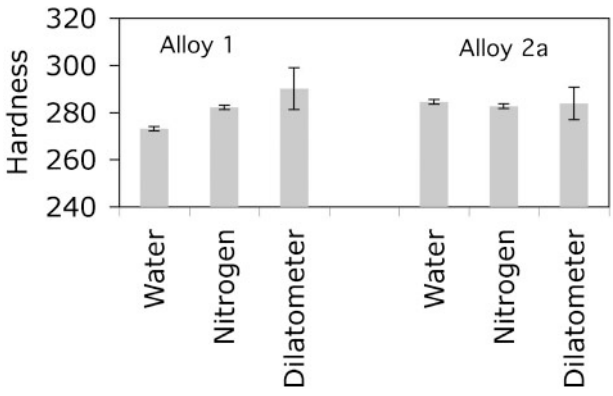

5 Vickers hardness (10 kg) measured on samples which were water quenched, quenched in liquid nitrogen and cooled in a dilatometer at 10 K s^{-1}: error bars represent range of measurements; notice exaggerated scale; differences in hardness between different samples are small

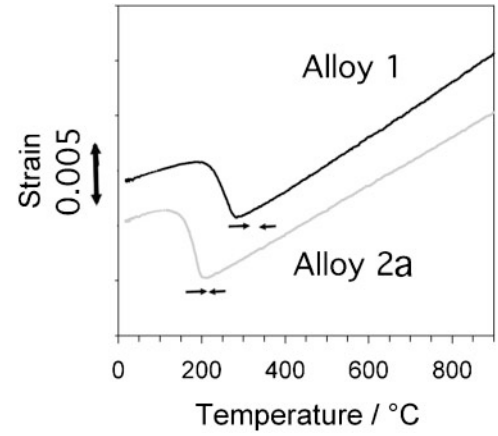

6 Dilatometric data: arrows indicate 95% confidence limits in determination of M_S temperature; for alloy 1, M_S is determined to be 327±13°C and for alloy 2a, 216±2°C

Experimental weld metals

Equilibrium phase diagram calculations indicate that alloy 2a should solidify completely to δ ferrite before its transformation into austenite (Fig. 3). It is, however, possible that solidification during welding occurs without equilibrium. For example, it is well known that austenitic solidification can occur if the cooling rate is large enough.[44–47] It is therefore essential to investigate the solidification microstructure in the welded state.

The investigation of actual weld metal was conducted in two stages, first using the cast alloy 2a to make a bare electrode for a single pass weld using the tungsten inert gas technique. After evaluating the results, a corresponding metal cored wire (alloy 2b) was manufactured in order to fabricate welds for distortion as well as mechanical property characterisations, as described later.

Small scale weld

The purpose of the first welding experiment was simply to assess the solidification microstructure using a small facility at the University of Cambridge. Samples of alloy 2a were used for arc welding two austenitic stainless steel plates (Table 1), the joint preparation being a V shape with a 90° included angle, penetrating half the thickness

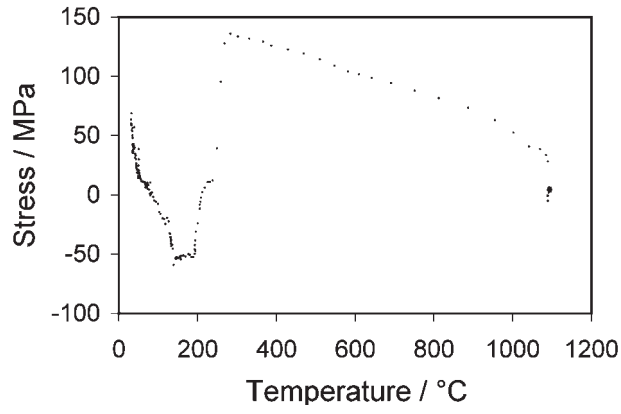

7 Satoh test on sample of alloy 2a, showing how transformation plasticity compensates for stress accumulated in constrained sample as it cools from austenitic phase

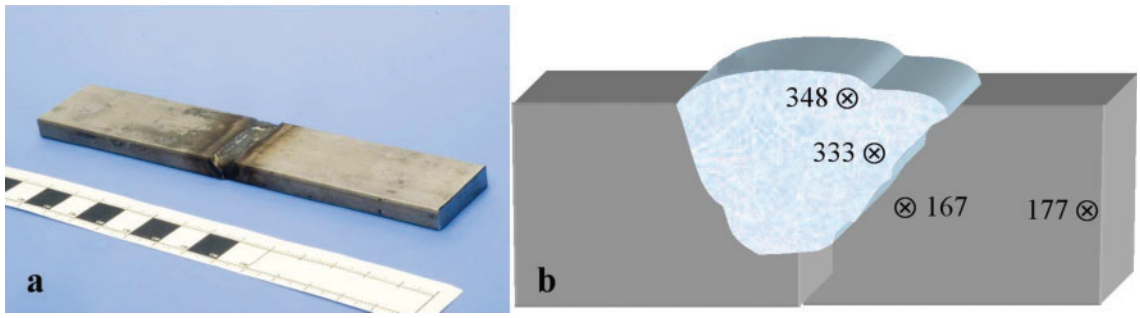

a stainless steel plates welded using conventional tungsten inert gas torch and alloy 2a as weld metal; *b* joint configuration and Vickers hardness data (10 kg load)

8 Single pass weld made in Cambridge using alloy 2a

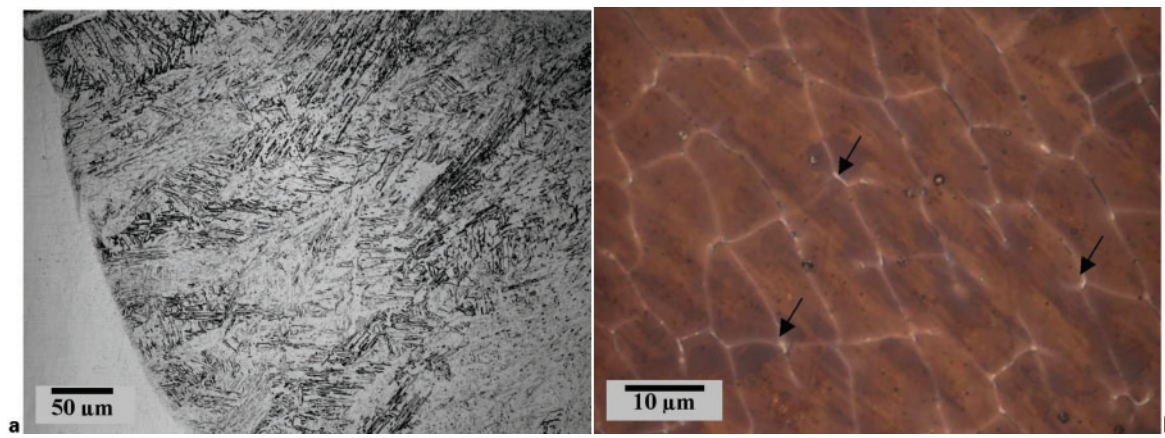

a essentially martensitic microstructure revealed by etching with Fry's reagent; *b* high magnification image showing small amount of discontinuous δ ferrite revealed by using Lichtenegger colour etching

9 Single pass weld made in Cambridge using alloy 2a

and with abutting surfaces on the lower half. The welding was carried out using a Murex 201i welder; this equipment does not allow the welding voltage to be monitored and the welding is conducted manually. It is not therefore possible to measure the heat input, but the welding current was 94 A, the welding speed was $\sim 0{\cdot}5$ mm s^{-1} (the open circuit voltage is 65 V). The final weld is illustrated in Fig. 8 and it was particularly noticeable that there was almost no distortion after the weld cooled and the plates were released from their clamps.

The welding process introduced some dilution in the weld metal (Table 1); the hardness of the weld deposit, in the range 333–348 HV, is consistent with a martensitic microstructure which is illustrated in Fig. 9*a*. It is also evident from Fig. 9*b* that the amount of δ ferrite left in the weld is too small to form a continuous network. This is important since networks of this kind are known to lead to poor toughness.

Larger welds

Metal cored wire (alloy 2b) was manufactured at ESAB AB (Sweden) with chemical composition intended to be similar to that of alloy 2a. The composition of alloy 2b in the as welded condition, using the gas tungsten arc technique, is listed in Table 1 as 'metal cored alloy 2b multipass weld'.

Distortion experiments

Distortion measurements were conducted by fabricating single pass square butt joints on 304L stainless steel base plates, and as an alternative, mild steel base plates, using the gas metal arc welding technique. Each of the base plates had dimensions $200 \times 50 \times 6$ mm. There was no opening at the butting surfaces before welding, and no clamping during welding to deposit a single bead using a heat input of 1 kJ mm^{-1} and a shielding gas of Ar + 2%CO_2. Note from Table 1 that there was no significant enhancement of carbon due to the use of CO_2 in the shielding gas. Table 2 and Fig. 10 show that the new welding consumable alloy 2b in all cases significantly minimises distortion when compared with a non-transforming austenitic weld metal (OK Autrod 308LSi).

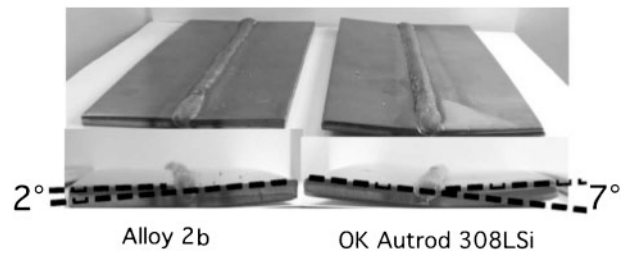

10 Deflection of 6 mm thick mild steel plates following single pass welding using martensitic alloy 2b used as consumable in one case and non-transforming austenitic welding wire OK Autrod 308LSi in the other

Mechanical properties

To assess the tensile and Charpy properties, all weld metal tests were done by preparing multipass welds in

Table 2 Measured angular distortions in butt welds prepared using alloy 2b, for comparison against commercial, non-transforming austenitic stainless steel welding wire, and laboratory variant of martensitic metal cored alloy: hardness of fusion zone following welding is also stated

		Angular distortion at start		Angular distortion at finish	
Welding wire	Wire diameter, mm	Austenitic base	Mild steel base	Austenitic base	Mild steel base
Alloy 2b welding wire	1·4	2·4°	1·7°	5·0°	2·0°
Austenitic OK Autrod 308LSi	1·2	5·5°	7·1°	5·2°	7·2°
Martensitic alloy	1·4	4·5°	4·3°	6·9°	4·2°
		Weld hardness, HV5			
		Austenitic base	Mild steel base		
Alloy 2b		200–225	330–345		
Austenitic OK Autrod 308LSi		160–175	360–385		

Table 3 All weld metal properties of alloy 2b and martensitic metal cored alloy, made using gas metal arc welding with Ar + 2%CO_2

	0·2% proof strength	Tensile strength	Elongation	Impact energy, J		Hardness, HV10					
						Whole weld			Last bead		
	MPa	MPa	%	20°C	−20°C	Min.	Mean	Max.	Min.	Mean	Max.
Alloy 2b	838	1069	17·6	72	53	317	342	369	321	335	346
Martensitic alloy	699	1094	15·8	57	52	323	341	355	323	339	348

the ISO 2560 geometry, again using the gas metal arc technique, on 20 mm thick mild steel plates which were buttered to reduce dilution effects. In each case, the weld consisted of a total of 13 beads, in six layers (three beads in the final layer), at 27 V, 302 A direct current and a welding speed of 45 cm min^{-1}, wire diameter 1·4 mm and a wire feed speed of 9·3 m min^{-1}. A shielding gas of Ar containing 2%CO_2 was used at a flow rate of 20 L min^{-1}. The interpass temperature was in the range 100–125°C.

The measured mechanical property data are listed in Table 3. It is seen that the properties of alloy 2b compare well with a commercial martensitic welding consumable, while its toughness at room temperature is significantly higher. The overall hardness was in the range 317–369 HV10 with an average of 342 HV10 (Table 3). The results show that there is no major variation in the hardness values of the different layers, primarily because the low carbon concentration ensures that tempering effects due to the heat pulses associated with multipass welding are minimised.[48]

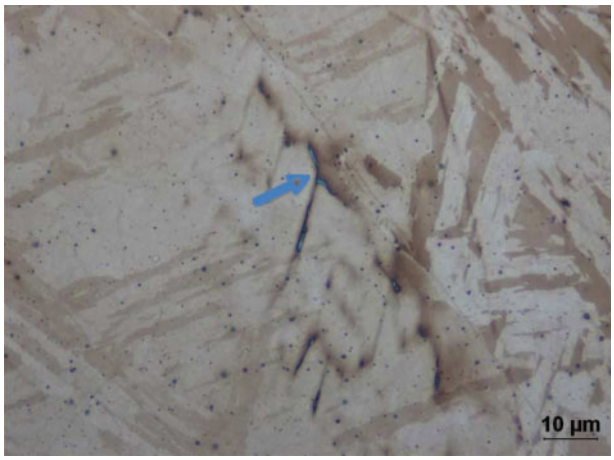

11 Alloy 2b multipass weld, etched using Kallings reagent: microstructure is predominantly martensitic with very small amount of δ ferrite indicated by arrow

Figure 11 shows the microstructure of the alloy 2b multipass weld, consisting essentially of martensite but with a very small amount of δ ferrite. There were no significant variations noted as a function of position within the fusion zone.

Conclusions

Stainless steel welding alloys have been designed with a view to minimising the distortion due to residual stresses that develop during the cooling of a welded assembly. The alloy design procedures have ensured solidification as δ ferrite, then transform almost completely into austenite and finally into martensite. The remnants of δ ferrite do not form continuous networks in the final microstructure, leading to good toughness. Furthermore, the martensite start temperature has been suppressed to about 220°C, a feature essential in order to ensure the accumulation of thermal contraction stresses following the exhaustion of the austenite. The transformation plasticity associated with the formation of martensite under the influence of the stresses that develop when a weld cools, has been shown experimentally to be capable of reducing the distortion in the final weld.

Work is now being initiated to characterise in detail, using neutron diffraction, the distribution of residual stress in welded plates.

Acknowledgements

We are grateful for support from the UK Ministry of Defence and also thank Håkan Arcini and Eva-Lena Berguist at ESAB AB (Sweden) for their technical support with the metallography and mechanical tests.

References

1. G. Digiacomo: 'Residual stresses in high-strength steel weldments and their dimensional stability during welding and stress relieving', *Mater. Sci. Eng.*, 1969, **4**, 133–145.
2. M. V. Deo and P. Michaleris: 'Prediction of buckling distortion of welded structures', *Sci. Technol. Weld. Join.*, 2003, **8**, 55–61.
3. M. V. Deo and P. Michaleris: 'Mitigation of welding induced buckling distortion using transient thermal tensioning', *Sci. Technol. Weld. Join.*, 2003, **8**, 79–88.
4. H. J. Zhang, G. J. Zhang and L. Wu: 'Effects of arc distance on angular distortion by asymmetrical double sided arc welding', *Sci. Technol. Weld. Join.*, 2007, **12**, 564–571.
5. P. Raman Venkata, G. Madhusudhan Reddy and T. Mohandas: 'Microstructure, hardness and residual stress distribution in maraging steel gas tungsten arc weldments', *Sci. Technol. Weld. Join.*, 2008, **13**, 388–394.
6. P. Wongpanya, Th. Bollinghaus, G. Lothongkum and Th. Kannengiesser: 'Effects of preheating and interpass temperature on stresses in S 1100 QL multi-pass butt-welds', *Weld. World*, 2008, **52**, 79–92.
7. N. Urabe, A. Yoshitake and H. Kagawa: 'Effect of welding residual stress on fatigue and fracture toughness', Proc. 4th Int. Symp. on 'Offshore mechanics and arctic engineering', Vol. 1, 190–195; 1985, New York, American Society of Mechanical Engineers.
8. H. V. Cordiano: 'Effect of residual stress on the low cycle fatigue life of large scale weldments in high strength steel', *J. Eng. Indust. ASME*, 1970, **92**, 86–92.
9. Y.-S. Yang, K.-J. Son, S.-K. Cho, S.-G. Hong, S.-K. Kim and K.-H. Mo: 'Effect of residual stress on fatigue strength of resistance spot weldment', *Sci. Technol. Weld. Join.*, 2001, **6**, 397–401.
10. W. K. C. Jones and P. J. Alberry: 'A model for stress accumulation in steels during welding', *Met. Technol.*, 1977, **11**, 557–566.
11. A. Ohta, N. Suzuki, Y. Maeda, K. Hiraoka and T. Nakamura: 'Superior fatigue crack growth properties in newly developed weld metal', *Int. J. Fatig.*, 1999, **21**, S113–S118.
12. A. Ohta, O. Watanabe, K. Matsuoka, C. Shiga, S. Nishijima, Y. Maeda, N. Suzuki and T. Kubo: 'Fatigue strength improvement by using newly developed low transformation temperature welding material', *Weld. World*, 1999, **43**, 38–42.
13. A. Ohta, N. Suzuki, and Y. Maeda: in 'Properties of complex inorganic solids 2', (ed. A. Meike), 401–408; 2000, New York, Kluwer Academic/Plenum Publishers.
14. P. J. Withers and H. K. D. H. Bhadeshia: 'Residual stress part 1 – measurement techniques', *Mater. Sci. Technol.*, 2001, **17**, 355–365.
15. P. J. Withers and H. K. D. H. Bhadeshia: 'Residual stress part 2 – nature and origins', *Mater. Sci. Technol.*, 2001, **17**, 366–375.
16. A. Ohta, K. Matsuoka, N. T. Nguyen, Y. Maeda and N. Suzuki: 'Fatigue strength improvement of lap welded joints of thin steel plate using low transformation temperature welding wire', *Weld. J. Res. Suppl.*, 2003, **82**, 77s–83s.
17. J. Eckerlid, T. Nilsson and L. Karlsson: 'Fatigue properties of longitudinal attachments welded using low transformation temperature filler', *Sci. Technol. Weld. Join.*, 2003, **8**, 353–359.
18. H. Lixing, W. Dongpo, W. Wenxian and Y. Tainjin: 'Ultrasonic peening and low transformation temperature electrodes used for improving the fatigue strength of welded joints', *Weld. World*, 2004, **48**, 34–39.
19. S. Zenitani, N. Hayakawa, J. Yamamoto, K. Hiraoka, Y. Morikage, T. Yauda and K. Amano: 'Development of new low transformation temperature welding consumable to prevent cold cracking in high strength steel welds', *Sci. Technol. Weld. Join.*, 2007, **12**, 516–522.
20. J. A. Francis, H. J. Stone, S. Kundu, R. B. Rogge, H. K. D. H. Bhadeshia, P. J. Withers and L. Karlsson: 'Transformation temperatures and welding residual stresses in ferritic steels', Proc. PVP 2007, 1–8; 2007, San Antonio, TX,ASME.
21. Ph. P. Darcis, H. Katsumoto, M. C. Payares-Asprino, S. Liu and T. A. Siewert: 'Cruciform fillet welded joint fatigue strength improvements by weld metal phase transformations', *Fatig. Fract. Eng. Mater. Struct.*, 2008, **31**, 125–136.
22. M. C. Payares-Asprino, H. Katsumoto and S. Liu: 'Effect of martensite start and finish temperature on residual stress development in structural steel welds', *Weld. J., Res. Suppl.*, 2008, **87**, 279s–289s.
23. H. Dai, J. A. Francis, H. J. Stone, H. K. D. H. Bhadeshia and P. J. Withers: 'Characterising phase transformations and their effects on ferritic weld residual stresses with X-rays and neutrons', *Metall. Mater. Trans. A*, 2008, **39A**, 3070–3078.
24. Y. Mikami, Y. Morikage, M. Mochizuki and M. Toyoda: 'Angular distortion of fillet welded T joint using low transformation temperature welding wire', *Sci. Technol. Weld. Join.*, 2009, **14**, 97–105.
25. H. K. D. H. Bhadeshia: 'Possible effects of stress on steel weld microstructures', in 'Mathematical modelling of weld phenomena – II', (ed. H. Cerjak and H. K. D. H. Bhadeshia), 71–118; 1995, London, Institute of Materials.
26. A. P. Bond: 'Mechanisms of intergranular corrosion in ferritic stainless steels', *Trans. Metall. Soc. AIME*, 1969, **245**, 2127–2134.
27. J. J. Demo and A. P. Bond: 'Intergranular corrosion and embrittlement of ferritic stainless steels', *Corrosion*, 1975, **31**, 21–22.
28. T. Sourmail, C. H. Too and H. K. D. H. Bhadeshia: 'Sensitisation and evolution of Cr-depleted zones in Fe–Cr–Ni–C systems', *ISIJ Int.*, 2003, **43**, 1814–1820.
29. J. G. Williams and F. J. Barbaro: 'Sensitisation and intergranular stress corrosion cracking of the HAZ of welded 12Cr ferritic stainless steels', *Austr. Weld. J.*, 2005, **50**, 34–48.
30. N. Suutala: 'Solidification of austenitic stainless steels', *Acta Univ. Ouluensis C*, 1983, **26C**, 53–60.
31. L. Myllykoski and N. Suutala: 'Effect of solidification mode on hot ductility of austenitic stainless steel', *Met. Technol.*, 1983, **10**, 453–460.
32. V. P. Kujanpää, S. A. David and C. L. White: 'Formation of hot cracks in austenitic stainless steel welds – solidification cracking', *Weld. J. Res. Suppl.*, 1986, **65**, 203s–212s.
33. L. Kaufman and M. Cohen: 'Thermodynamics and kinetics of martensitic transformation', *Prog. Met. Phys.*, 1958, **7**, 165–246.
34. H. K. D. H. Bhadeshia: 'The driving force for martensitic transformation in steels', *Met. Sci.*, 1981, **15**, 175–177.
35. H. K. D. H. Bhadeshia: 'Thermodynamic extrapolation and the martensite-start temperature of substitutionally alloyed steels', *Met. Sci.*, 1981, **15**, 178–150.
36. G. Ghosh and G. B. Olson: 'Kinetics of FCC→BCC heterogeneous martensitic nucleation', *Acta Metall. Mater.*, 1994, **42**, 3361–3370.
37. T. Cool and H. K. D. H. Bhadeshia: 'Prediction of the martensite-start temperature of power plant steels', *Mater. Sci. Technol.*, 1996, **12**, 40–44.
38. NPL MTDATA Software, National Physical Laboratory, Teddington, UK, 2006.
39. D. Carrouge, H. K. D. H. Bhadeshia and P. Woolin: 'Microstructural change in high T HAZ of low carbon weldable 13Cr martensitic stainless steels', *Stainless Steel World*, Oct. 2003, 16–23.
40. D. Carrouge, H. K. D. H. Bhadeshia and P. Woolin: 'Effect of δ-ferrite on impact properties of supermartensitic stainless steel heat affected zones', *Sci. Technol. Weld. Join.*, 2004, **9**, 377–389.
41. H.-S. Yang and H. K. D. H. Bhadeshia: 'Uncertainties in the dilatometric determination of the martensite-start temperature', *Mater. Sci. Technol.*, 2007, **23**, 556–560.
42. H.-S. Yang and H. K. D. H. Bhadeshia: 'Designing low-carbon, low-temperature bainite', *Mater. Sci. Technol.*, 2008, **24**, 335–342.
43. K. Satoh: 'Transient thermal stresses of weld heat-affected zone by both-ends-fixed bar analogy', *Kovove Mater.*, 1970, **8**, 569–587.
44. J. M. Vitek, A. Dasgupta and S. A. David: 'Microstructural modification of austenitic stainless steels by rapid solidification', *Metall. Trans. A*, 1983, **14A**, 1833–1841.
45. J. W. Elmer, S. M. Allen and T. W. Eagar: 'Microstructural development during solidification of stainless steel alloys', *Metall. Trans. A*, 1989, **20A**, 2117–2131.
46. H. K. D. H. Bhadeshia, S. A. David and J. M. Vitek: 'Solidification sequences in stainless steel dissimilar alloy welds', *Mater. Sci. Technol.*, 1991, **7**, 50–61.
47. S. Tsukamoto, H. Harada and H. K. D. H. Bhadeshia: 'Metastable phase solidification in electron beam welding of dissimilar stailess steel', *Mater. Sci. Eng. A*, 1994, **A178**, 189–194.
48. G. R. Speich and W. C. Leslie: 'Tempering of steel', *Metall. Trans.*, 1972, **3**, 1043–1054.